journal

J. Am. Ceram. Soc., 95 [9] 2801–2807 (2012)
DOI: 10.1111/j.1551-2916.2012.05253.x

Highly Transparent AlON Pressurelessly Sintered from Powder Synthesized by a Novel Carbothermal Nitridation Method

Xihai Jin, Lian Gao,*,† Jing Sun, Yangqiao Liu, and Linhua Gui

The State Key Laboratory on High Performance Ceramics and Superfine Microstructure, Shanghai Institute of Ceramics, Shanghai 200050, China

Transparent AlON was pressurelessly sintered from powders synthesized by a two-step carbothermal nitridation method, using core-shell structured Al_2O_3/C mixture derived from the pyrolysis of an Al_2O_3/ureaformaldehyde-resin nanocomposite precursor as the starting material. It was found that the amorphous carbon layer on the Al_2O_3 particle surface could strongly retard the coalescence and growth of Al_2O_3 particles during the carbothermal nitridation process. As a result, the formation temperature and particle size of the AlON powder were significantly reduced. The AlON powder synthesized showed a bimodal particle size distribution at 0.2 and 0.7 μm and was well dispersed; its maximum particle size was below 0.9 μm. Under the aid of proper sintering additive, transparent AlON ceramics with an average in-line transmittance above 80% at visible to infrared range were obtained through pressureless sintering.

I. Introduction

Transparent aluminum oxynitride (AlON) ceramics possesses many interesting properties, such as robust mechanical strength, good chemical attack resistance, and good transparency from ultraviolet to mid-infrared range, which make it an ideal candidate for transparent armor, missile dome, and optoelectronic window, etc.[1] However, there is great difficulty in sintering of the material. Up to now, most of the transparent AlON are prepared by hot pressing or hot isostatic pressing techniques.[2–5] The high cost of these techniques limits it from large scale commercial production. Although there are a few reports on the pressureless sintering of transparent AlON,[6–9] the sintering temperatures are very high, sometimes even up to 2000°C. Till now, pressureless sintering of transparent AlON is still a challenge. To solve the problem, fine AlON powder of high sinterbility is desired.

At present, many methods have been developed for AlON powder synthesis. Among them, carbothermal nitridation and solid-state reaction methods are most widely used[6,10–14] because of their advantages in cost and simplicity. However, restricted by thermodynamic reason, AlON cannot be formed at temperatures below 1640°C.[15] During the heating process of AlON synthesis, extensive coalescence and growth of Al_2O_3 particles will occur in the Al_2O_3/C or Al_2O_3/AlN starting powders, which makes the subsequent AlON formation more difficult and significantly elevates the synthesizing temperature. In consequence, current AlON powders are mostly synthesized at temperature above 1750°C, sometimes even at 1825°C.[6,11–14] The powders obtained are generally seriously aggregated, with particle size from several to over 10 μm. The poor sinterbility of the powder is unfavorable for the pressureless sintering of transparent AlON.

Recently, core-shell structured powders composed of inorganic particles that were surface coated with carbon nanolayers were reported.[16] These powders were synthesized through *in situ* polymerization of organic polymers on inorganic particle surfaces followed by low temperature pyrolysis. If core-shell structured Al_2O_3/C powder can be prepared by this method and used for AlON synthesis through carbothermal nitridation, the coalescence and growth of Al_2O_3 particles during the heating stage of AlON synthesis will be effectively retarded. Hereby, a significant reduction in the AlON formation temperature and its particle size can be expected. This cast a new light on the synthesis of fine AlON powder.

On the basis of above assumption, fine AlON powder was synthesized through a two-step carbothermal nitridation method in the present work, using core-shell structured Al_2O_3/C powder that was converted from the *in situ* polymerized Al_2O_3/UFR (ureaformaldehyde resin) nanocomposite precursor as the starting material. It was found that highly transparent AlON could be pressurelessly sintered from this powder at a temperature range from 1920°C to 1950°C under the aid of MgO, Y_2O_3, and La_2O_3 sintering additives.

II. Experimental Procedure

(1) Synthesis of Al_2O_3/UFR Nanocomposite Precursor and AlON Powder

High purity nanosized γ-Al_2O_3 (AKP-G015, Sumitomo Chemical Co. Ltd., Tokyo, Japan), urea and formaldehyde were used as the starting materials for the synthesis of Al_2O_3/UFR precursor. First, 50 g nanosized γ-Al_2O_3 was dispersed in 1000 mL distilled water, then 21.2 g formaldehyde and 21.9 g urea were added in sequence. After refluxed at 95°C for 5 h at pH 2–3 and vacuum dried at 120°C, core-shell structured Al_2O_3/UFR nanocomposite precursor was obtained through the *in situ* polymerization of urea and formaldehyde on Al_2O_3 particle surface.

The Al_2O_3/UFR precursor was pyrolyzed at 800°C in high purity argon (99.999%, oxygen < 2 ppm), ground with Al_2O_3 mortar and then screened through 200 mesh sieve. The resulting fine Al_2O_3/C mixture was used for AlON synthesis through a two-step carbothermal nitridation method in nitrogen. During the carbothermal nitridation process, the Al_2O_3/C mixture was first heat treated at a relatively low temperature of 1500°C–1600°C for 2 h, so that a fine Al_2O_3/AlN intermediate product could form. Then, the intermediate product was continuously heat treated at a higher temperature of 1680°C–1720°C for 2 h to induce AlON formation through the solid-state reaction between Al_2O_3 and AlN. Finally, the AlON powder obtained was slightly ball milled for 2 h and calcined at 650°C for 1 h in air to remove the aggregates and possible carbon residues in it before later use.

H.-J. Kleebe—contributing editor

Manuscript No. 30628. Received November 07, 2011; approved April 05, 2012.
*Member, The American Ceramic Society.
†Author to whom correspondence should be addressed. e-mail: liangao@mail.sic.ac.cn

(2) Fabrication of Transparent AlON

The AlON powder prepared above was mixed simultaneously with suitable amounts of $Mg(NO_3)_2$, $Y(NO_3)_3$ and $La(NO_3)_3$, followed by forming into pellets of 20 mm in diameter and 5 mm in thickness through cold isostatic pressing at 200 MPa. The amount of $Mg(NO_3)_2$, $Y(NO_3)_3$, and $La(NO_3)_3$ additives was strictly controlled to give MgO, Y_2O_3, and La_2O_3 dopant levels of 0.1, 0.08, and 0.025 wt%, respectively, according to the solubility limits of Mg, Y, and La in AlON reported by Miller.[17] The pellet was embedded in a powder bed of the same chemical composition as its own, and pressurelessly sintered in a graphite furnace at 1920°C–1950°C for 8 h under nitrogen atmosphere at a heating rate of 8°C/min. The sintered samples were ground and mirror polished on both sides to a thickness of 1 mm for optical property measurement.

(3) Characterization

The infrared spectrum of the Al_2O_3/UFR nanocomposite precursor was recorded on a Fourier Transform Infrared Spectrometer (EQUINOX55, Bruker Optics, Ettlingen, Germany). The weight loss during pyrolysis of the precursor in argon was monitored by thermogravimetric analysis (TG; STA449C, NETZSCH, Selb, Germany) at a heating rate of 10°C/min. The total carbon content of the pyrolyzed product was analyzed by inductively coupled plasma atomic emission spectroscopy method (ICP-AES, Vista AX, Varian Inc., Palo Alto, CA). The particle morphology and particle chemical composition of the Al_2O_3/UFR precursor and the pyrolyzed product were characterized on a transmission electron microscope (TEM; JEM-2010, JEOL, Tokyo, Japan) that is equipped with an Oxford ISIS X-ray EDS microanalysis system (Oxford Instruments, Oxfordshire, UK). For particle morphology observation, a hole-free carbon film was used as the sample support. While for energy dispersive spectroscopy (EDS) analysis, a lacy carbon film was used as the sample support, and the chemical composition of the particles that were not in close proximity of the carbon support were analyzed to eliminate the noise signal from the support film.

The phase composition of the synthesized AlON powder as well as the intermediate products formed during the two-step carbothermal nitridation process was characterized by X-ray diffractometry (XRD; D/MAX-RBX, Rigaku, Osaka, Japan). The powder morphology was observed by TEM and scanning electronic microscopy (SEM; JEOL, JSM-6390, Japan). The particle and/or aggregate size distribution of the AlON powder was measured on a Brookheaven Zetaplus particle size analyzer (Brookheaven Instruments Corporation, NY). The in-line transmittance of the transparent AlON ceramics was measured over the wavelength range from 200 to 2000 nm, using a Cary 5000 UV-Vis-NIR type spectrophotometer (Varian Inc., Palo Alto, CA).

III. Results and Discussion

Figure 1 shows the infrared spectrum of the Al_2O_3/UFR nanocomposite precursor, whereas the assignment of the absorption bands in it are specified in Table I.[18–20] It can be seen that the absorption bands in the spectrum can be roughly categorized into two sets, according to the difference in their origins. The first set of bands, which appeared at 3367, 1631, 1566, 1385, 1254, and 1041 cm^{-1}, agreed very well with the characteristic adsorption bands of various organic groups in UFR[18,19]; whereas the second set of bands, which appeared at 810, 756, 630, and 571 cm^{-1}, agreed well with the characteristic adsorption bands of the AlO_4 and AlO_6 units in γ-Al_2O_3.[20] The whole spectrum can be regarded as a superimposition of the infrared spectra of UFR and γ-Al_2O_3. This indicates that Al_2O_3/UFR nanocomposite has been successfully synthesized through *in situ* polymerization of urea and formaldehyde in the Al_2O_3 suspension.

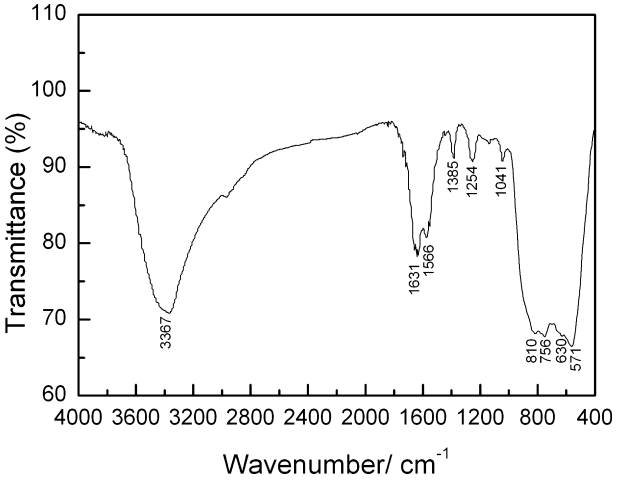

Fig. 1. Infrared spectrum of the Al_2O_3/UFR nanocomposite precursor.

Table I. Probable Assignments of the Adsorption Bands in the IR Spectrum of Al_2O_3/UFR Precursor

	Band position (cm^{-1})	Probable assignment
UFR	3367	ν N–H vibration in 2°-amine
	1631	ν C = O vibration in–$CONH_2$ (amide I)
	1566	NH-bending vibration (NH–CO) in 2°-amine (amide II)
	1385	CH bending vibration in CH_2/CH_2OH/N–CH_2–N
	1254	Amide III
	1041	ν C–O vibration of ether
γ-Al_2O_3	810	AlO_4 stretching
	756	AlO_4 stretching
	630	AlO_6 stretching
	571	AlO_6 stretching

Figure 2(a) shows the TEM image of the original γ-Al_2O_3 powder. Most of the particles in it took a needle-like morphology, which was typical of γ-Al_2O_3, while other particles were irregular shaped ones. In comparison with the needle-like particles, the irregular shaped particles were generally smaller in size. Figure 2(b) shows the TEM image of the Al_2O_3/UFR nanocomposite precursor. Most of the Al_2O_3 particles were homogeneously distributed in UFR matrix after the formation of Al_2O_3/UFR nanocomposite precursor. Due to the difference in contrast between Al_2O_3 and UFR, the Al_2O_3 particles were clearly distinguishable, especially for the larger needle-like ones. High-resolution transmission electron microscopy (HRTEM) and EDS examination of some isolated needle-like particles found that they all possessed core-shelled structures, with Al_2O_3 core and UFR shell [Figs. 2(c–e)]. The formation mechanism of such core-shell structured Al_2O_3/UFR particle can be understood as follows.

It is generally acknowledged that the surfaces of Al_2O_3 particles exposed to atmospheric moisture are terminated with a monolayer of hydroxyl groups[21] because of the surface hydrolysis effect. This should also hold for Al_2O_3 particles dispersed in water as in the present work. As the hydroxyl groups on Al_2O_3 particle surface showed a modestly strong basicity, they could readily react with formaldehyde through base-acid interaction.[22,23] As a result, strong bond between Al_2O_3 particle and formaldehyde was formed. At the later stage of Al_2O_3/UFR precursor synthesis, these surface-bonded formaldehyde molecules would work as coupling agent, which facilitated the *in situ* polymerization of

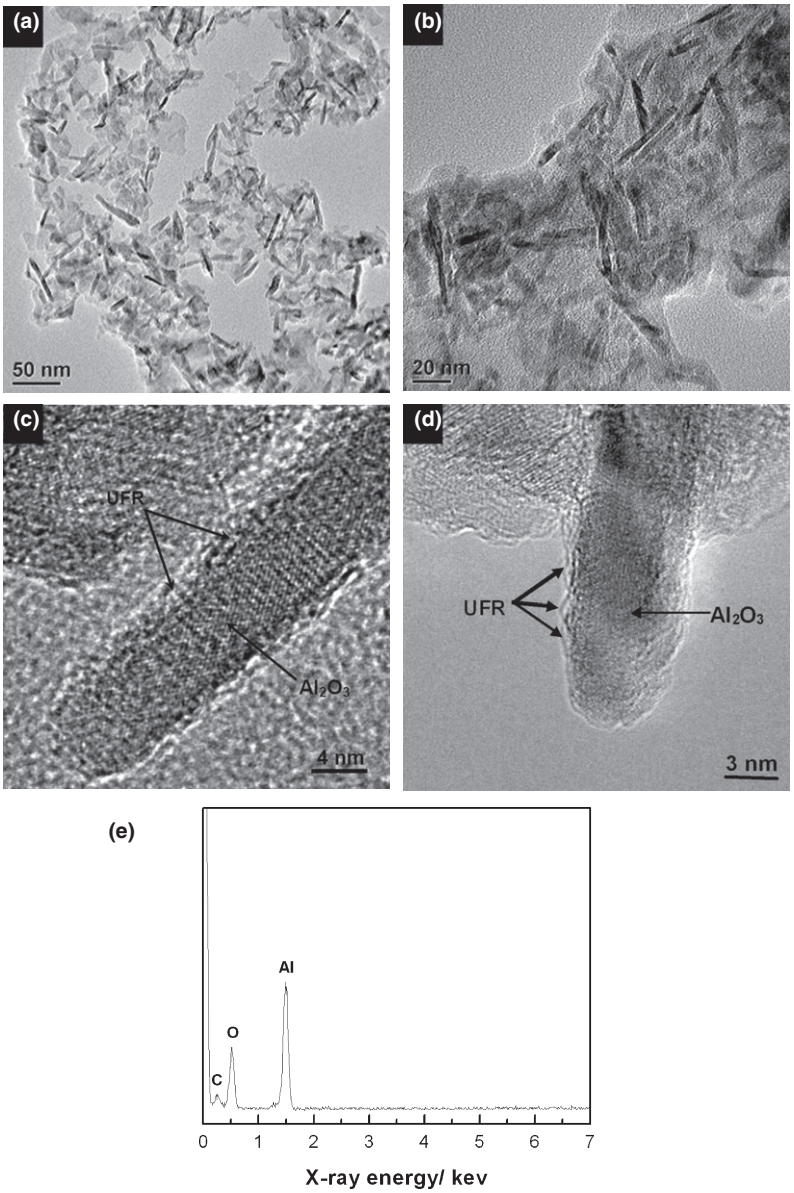

Fig. 2. TEM images of (a) the original γ-Al_2O_3 and (b) Al_2O_3/UFR precursor, (c–e) the HRTEM image and EDS spectrum of a needle-like Al_2O_3/UFR particle. The samples shown in image (a-c) were supported on a hole-free carbon film, whereas the sample shown in image (d) was supported on a lacy carbon film.

urea and formaldehyde on Al_2O_3 particle surface. Hereby, Al_2O_3 particles with surface-coated UFR could be formed.

Figure 3 shows the thermogravimetry (TG) and differential thermogravimetry (DTG) curves of the Al_2O_3/UFR nanocomposite precursor during its pyrolysis in argon. A sharp weight loss of about 27 wt% was observed at a narrow temperature range from 170°C to 350°C. Beyond this temperature range, the weight loss rate gradually slowed down. The weight loss continued up to 950°C, which was the upper temperature limit here. Such a weight loss behavior was nearly identical to that of pure UFR, as found by many previous researchers.[24,25] According to Jiang, the sharp weight loss at 170°C–350°C should be related with the rapid degradation of organic structures in UFR, whereas the slow weight loss at higher temperature should be related with further cracking of the degraded residues.[24] Both of these processes were accompanied by weight loss due to the concurrent release of gas species from the sample, which included H_2O, NH_3, HCN, CO_2, and HNCO, etc.

The Al_2O_3/C mixture obtained through the pyrolysis of the Al_2O_3/UFR precursor was in deep black and had a carbon content about 5.9–6.1 wt%. TEM observation indicated

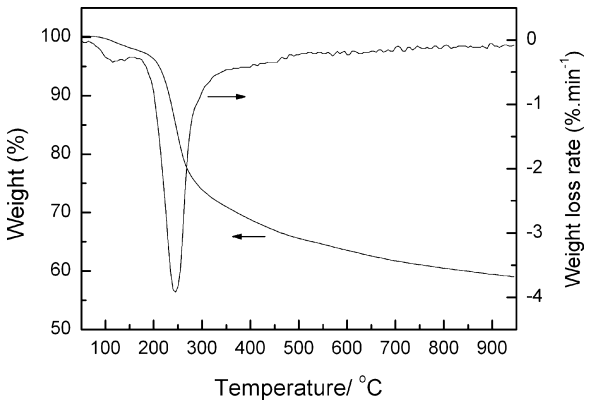

Fig. 3. TG/DTG curves of the Al_2O_3/UFR nanocomposite precursor.

that it showed nearly the same structure as the Al_2O_3/UFR precursor, except that UFR was replaced with carbon here [Fig. 4(a)]. Furthermore, a close examination of some iso-

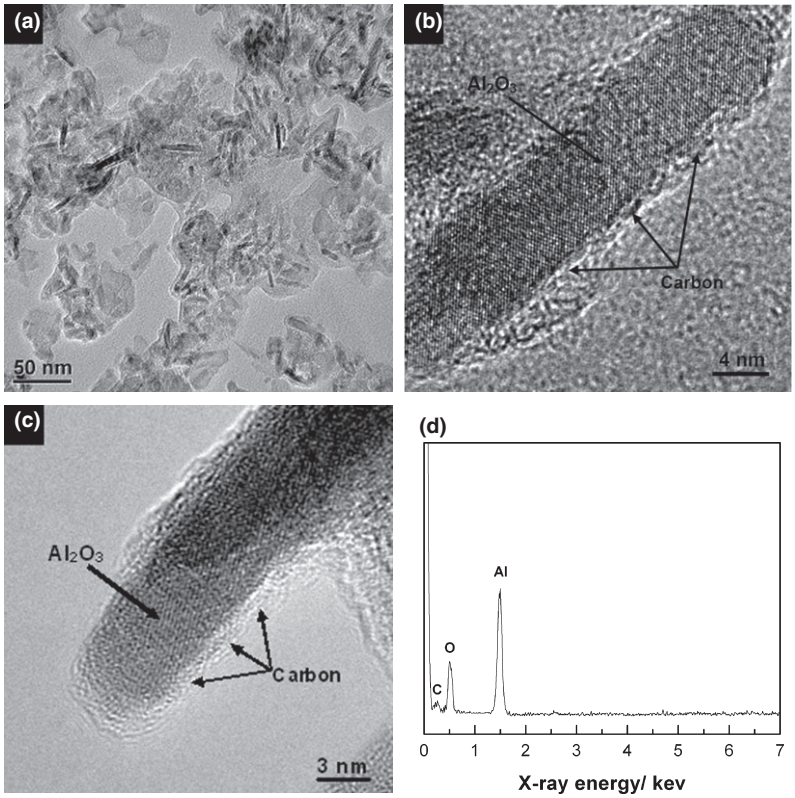

Fig. 4. (a–c) TEM and HRTEM images of the pyrolyzed Al_2O_3/C mixture and the needle-like Al_2O_3/C particles, (d) EDS spectrum of the needle-like Al_2O_3/C particle shown in image (c). The samples shown in image (a) and (b) were supported on a hole-free carbon film, whereas the sample shown in image (c) was supported on a lacy carbon film.

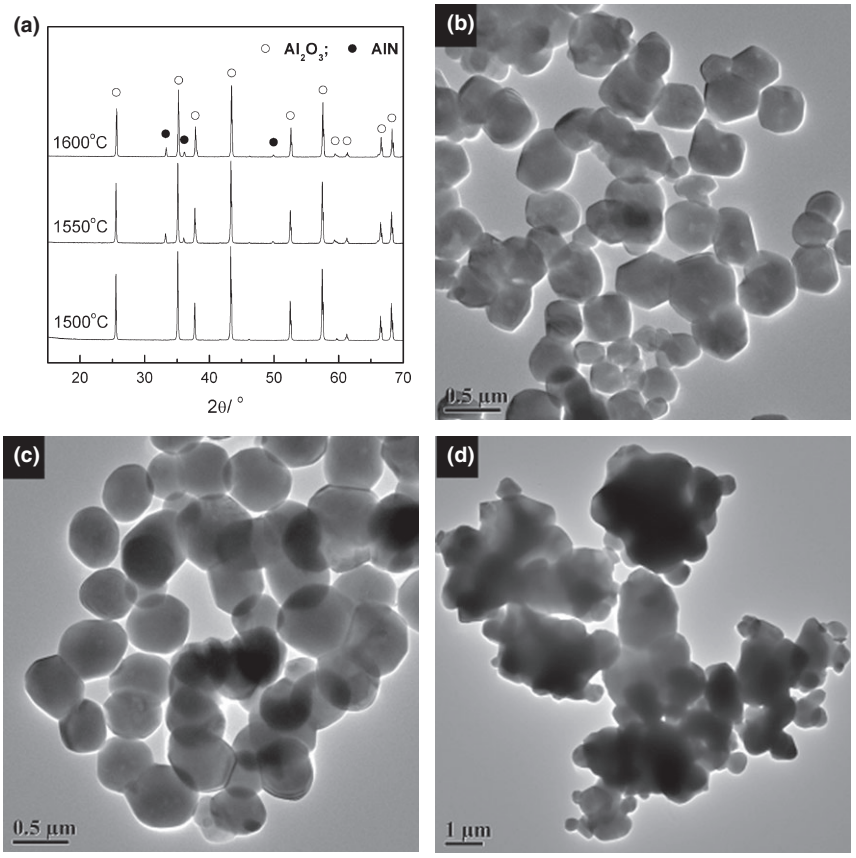

Fig. 5. (a) XRD patterns and (b, c) TEM images of the intermediate products that were formed after the first step heat treatment of the Al_2O_3/C mixture at different temperatures during AlON synthesis; (d) TEM image of an Al_2O_3 powder synthesized by calcining pure γ-Al_2O_3 powder at 1500°C.

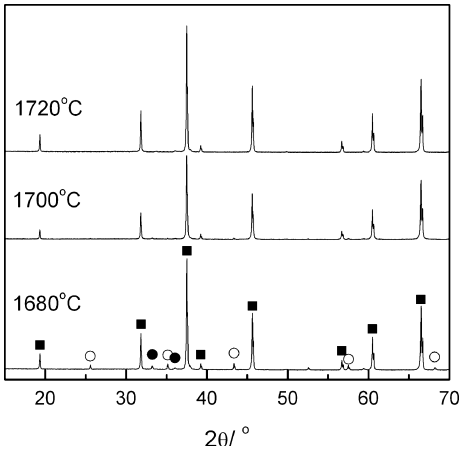

Fig. 6. XRD patterns of the AlON powders synthesized by two-step carbothermal nitridation method at different temperatures. The symbol ■, ○, and ● represent AlON, α-Al_2O_3, and AlN, respectively.

lated needle-like particles with HRTEM and EDS found that they also showed a core-shelled structure, possessing Al_2O_3 core and amorphous carbon shell [Figs. 4(b–d)]. This implied that the core-shelled structure of the Al_2O_3/UFR precursor particle was well preserved after its pyrolysis in argon.

Using the Al_2O_3/C mixture as starting material, AlON powder was synthesized through a two-step carbothermal nitridation method in nitrogen. Figure 5(a) shows the XRD patterns of the intermediate products that were obtained after the first step heat treatment of the Al_2O_3/C mixture at various temperatures. It was found that no chemical reaction occurred in the sample at temperature below 1500°C. However, when the temperature was increased to 1550°C, carbothermal nitridation reaction occurred. At this time, part of Al_2O_3 reacted with carbon and nitrogen, which led to the formation of AlN. In addition, it seemed that the AlN formation had almost completed at this temperature, further increase in temperature to 1600°C led to no obvious variation in the XRD pattern.

The intermediate products obtained at 1500°C and 1550°C were oxidized in air at 650°C to remove any possible residual carbon, and the resulting Al_2O_3 and Al_2O_3/AlN powders were characterized with TEM as shown in Figs. 5(b) and (c), respectively. For comparison, an Al_2O_3 powder that was obtained by calcining the pure nanosized γ-Al_2O_3 at 1500°C for 2 h in nitrogen was also presented in Fig. 5(d). It can be seen that the Al_2O_3 and Al_2O_3/AlN intermediate products showed spherical particle morphology and were fairly uniform; the average particle sizes of them were about 0.3 and 0.4 μm, respectively. In comparison with the Al_2O_3 powder synthesized from pure γ-Al_2O_3, which showed a wide particle size range of 0.5–3 μm and was seriously aggregated, the Al_2O_3 and Al_2O_3/AlN intermediate products were much finer and more uniform. Such a difference in powder morphologies was a direct evidence for the retarded growth and coalescence of Al_2O_3 particles during the heating stage of carbothermal nitridation process as explained below.

Due to the formation of core-shell structured Al_2O_3/C particles, the Al_2O_3 particles in the Al_2O_3/C mixture were separated from each other by refractory carbon, which led to a strong retarding effect on the coalescence and growth of Al_2O_3 particles during the carbothermal nitridation process. As a result, fine Al_2O_3 and Al_2O_3/AlN intermediate products were formed despite of the relatively high heat treatment temperatures. The formation of fine Al_2O_3/AlN intermediate product should be greatly helpful for reducing the AlON formation temperature and hereby its particle size during the subsequent second step heat treatment of AlON synthesis.

Figure 6 shows the XRD patterns of the AlON powders that were synthesized by the two-step carbothermal nitridation method, with a first step heat treatment at 1550°C and a second step heat treatment at 1680°C–1720°C. Although tiny amounts of Al_2O_3 and AlN impurity phases still remained in the powder synthesized at 1680°C because of the incomplete

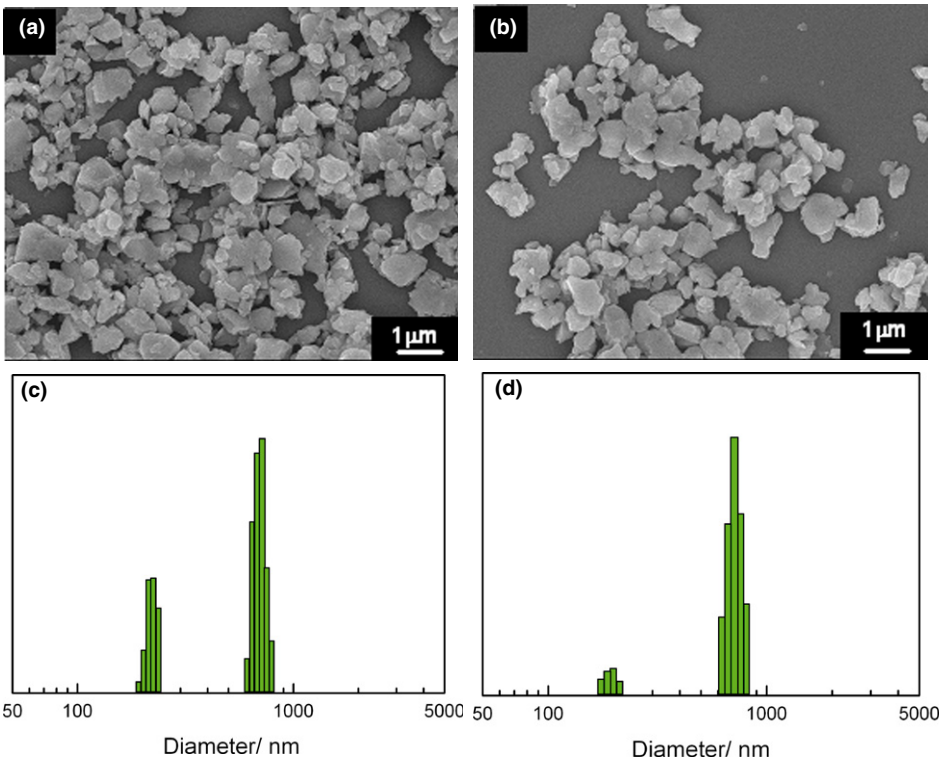

Fig. 7. SEM images and particle size distribution of AlON powders synthesized at (a, c) 1700°C and (b, d) 1720°C.

solid state reaction between Al_2O_3 and AlN, nearly pure AlON were formed for the powders synthesized at 1700°C and 1720°C. In comparison with the previous researches, where mechanically mixed Al_2O_3/C and Al_2O_3/AlN were used for AlON synthesis,[6,11–14] the AlON synthesis temperature here was about 50°C–100°C lower. The AlON powders obtained were nearly snow white in appearance and could be easily fractured with bare hands, X-ray photoemission spectroscopy (XPS) measurement found no residual carbon in them after air oxidation at 700°C. This means that the residual carbon content in the post-oxidized powders, if any, was very low and probably below the detecting limit of the instrument (100 ppm).

Figure 7 shows the SEM images and particle size distribution of the AlON powders that were synthesized at 1700°C and 1720°C. Both powders possessed a similar bimodal particle size distribution at 0.2 and 0.7 μm and were relatively well dispersed, their maximum particle sizes were both below 0.9 μm. The only obvious difference between them was that the powder synthesized at 1700°C was populated with more small sized particles than the one synthesized at 1720°C, due to its relatively lower synthesis temperature. To our knowledge, AlON powder of such small particle size has seldom been reported before.

Under the aid of MgO, Y_2O_3, and La_2O_3 sintering additives, transparent AlON ceramics was prepared through pressureless sintering, using the AlON powder synthesized at 1700°C. Figure 8(a) shows the optical image of the samples sintered at 1920°C and 1950°C. It can be seen that both samples were highly transparent, the text underlying them could be clearly seen. XPS measurement indicated that due to the protecting effect of the AlON embedding powder, no carbon contamination occurred in the samples, despite that they were sintered in a graphite furnace. In-line transmittance measurement indicated that the optical property of the sample sintered at 1950°C was relatively superior to that of the sample sintered at 1920°C [Fig. 8(b)]. Taking the in-line transmittance at 2000 and 350 nm as examples, the sample sintered at 1950°C showed respective in-line transmittance of 83.6% and 76%, whereas the sample sintered at 1920°C showed respective in-line transmittance of 80% and 60.3% at these two wavelengths; the in-line transmittance of the former sample was not only higher but also less wavelength dependent in comparison with that of the latter.

Furthermore, to clarify the degree of transparency of these samples, the relative in-line transmittance (RIT) of them were calculated, using the refractive index (n) of AlON reported by Hartnett[26]:

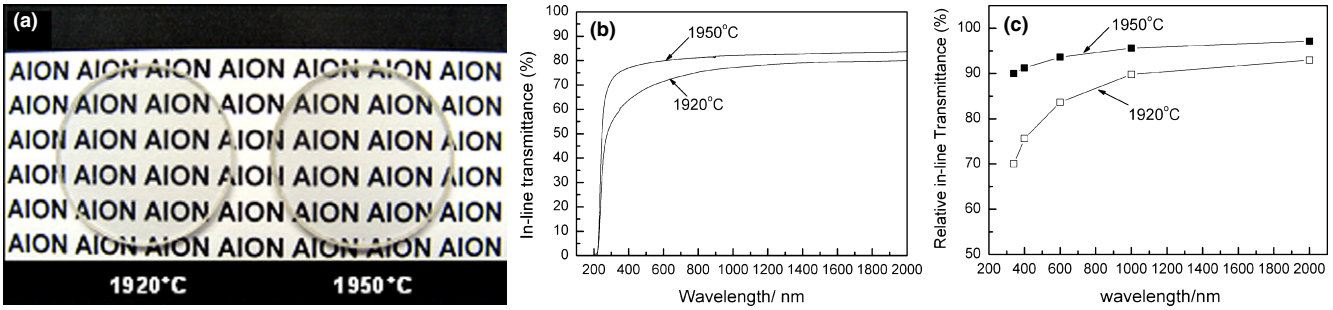

Fig. 8. (a) Optical images, (b) in-line transmittance, and (c) relative in-line transmittance of the transparent AlON sintered at 1920°C and 1950°C.

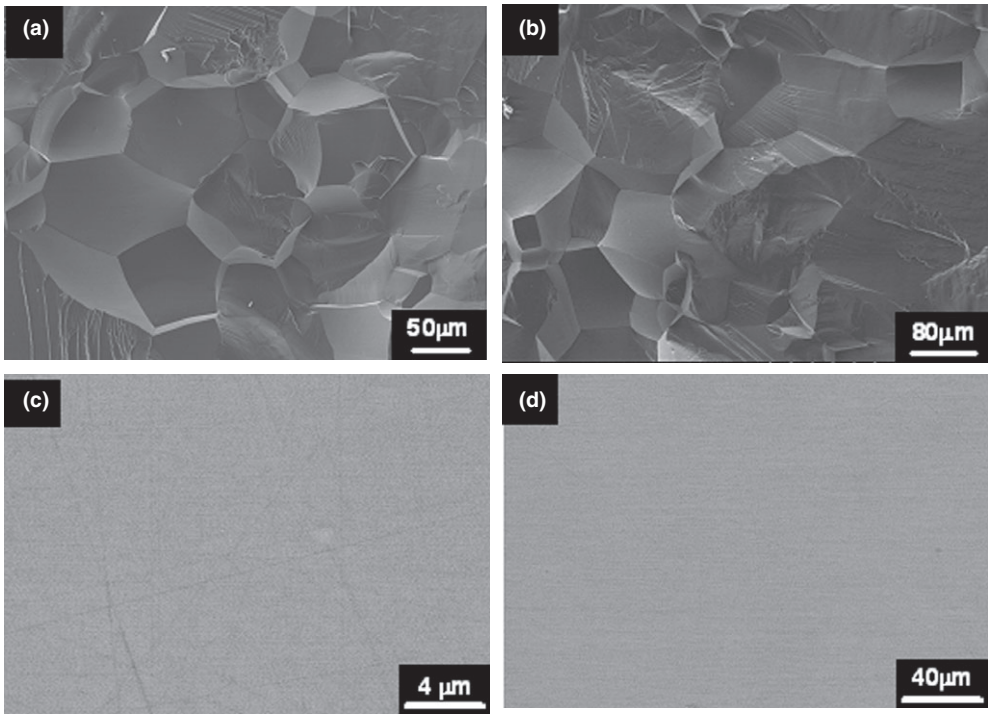

Fig. 9. (a, b) SEM images of the fracture surfaces of the AlON samples sintered at (a) 1920°C, and (b) 1950°C, (c, d) Backscattered SEM images of the polished surface of the sample sintered at 1920°C.

$$\mathrm{RIT} = \frac{\mathrm{MIT}}{\mathrm{TIT}} \tag{1}$$

$$\mathrm{TIT} = 1 - R_s = 1 - \frac{2\left(\frac{n-1}{n+1}\right)^2}{1 + \left(\frac{n-1}{n+1}\right)^2} \tag{2}$$

where R_s represents the reflection losses at the two sample surfaces at normal incidence, MIT and TIT represent the measured and theoretical in-line transmittance, respectively.[27] Figure 8(c) shows the results of the calculation. The RIT of the sample sintered at 1950°C was as high as 97.1% at a wavelength of 2000 nm, which meant that the in-line transmittance of the sample nearly reached its theoretical value and the sample was almost fully transparent at this wavelength. Although the RIT dropped slightly at shorter wavelengths, it still remained at a high level of above 90% at 350 nm. With respect to the sample sintered at 1920°C, it showed high RIT above 90% at wavelength above 1000 nm. Below this wavelength, the RIT decreased steadily to 70% at 350 nm. Anyway, the optical property of the sample was still fairly good, although it was inferior to that of the sample sintered at 1950°C.

Figures 9(a) and (b) shows the SEM images of the fracture surfaces of the sintered samples. Due to the prolonged heating at high temperature, both samples possessed coarse-grained microstructures. The grain sizes were in the range of 80–100 and 120–200 μm for the samples sintered at 1920°C and 1950°C, respectively. In addition, backscattered SEM images of the polished surface of the sample sintered at 1920°C indicate that this sample was highly densified and the sintering additives have almost completely dissolved into AlON grains. As a result, no residual pores and secondary phases formed from sintering additives could be observed in it [Figs. 9(c) and (d)]. Similar phenomena were also observed for the sample sintered at 1950°C, although the results were not given here. The absence of obvious pores and secondary phases within these samples caused a significant decrease in light scattering, thus transparent AlON of excellent optical property could be obtained. In fact, the in-line transmittance of the sample sintered at 1950°C has become comparable to that of the hot isostatically pressed transparent AlON,[3] and was much higher than the in-line transmittance of most of the pressurelessly sintered ones.[7,8,28]

IV. Conclusions

In summary, core-shell structured Al_2O_3/C mixture was synthesized through the pyrolysis of Al_2O_3/UFR nanocomposite precursor that was prepared by an *in situ* polymerization method. During the subsequent carbothermal nitridation process, the growth of Al_2O_3 particles was effectively retarded by the amorphous carbon layer on its surface, which led to a significant decrease in the formation temperature of AlON. As a result, fine AlON powder with a particle size in submicrometer range was obtained. This powder was well sinterable, and under the aid of MgO, Y_2O_3, and La_2O_3 sintering additive, highly transparent AlON ceramics with an in-line transmittance above 80% at visible to infrared range could be prepared through pressureless sintering.

Acknowledgments

This work was supported by the National Natural Science Foundation of China (50672112) and the Key Project for Fundamental Research of Shanghai (09JC1415400).

References

[1]J. W. McCauley, P. Patel, M. Chen, G. Gilde, E. Strassburger, B. Paliwal, K. T. Ramesh, and D. P. Dandekar, "AlON: A Brief History of its Emergence and Evolution," *J. Eur. Ceram. Soc.*, **29**, 223–36 (2009).

[2]T. M. Hartnett and J. M. Wahl, "Method of Making Aluminum Oxynitride and Aluminum Oxynitride Prepared by the Method"; W.O. Pat. No. 02/06156 A1, Jan. 24, 2002.

[3]A. Fujii and K. Shibata, "Transparent Aluminum Oxynitride Ceramics and the Method of Manufacture"; JP Pat. No. 3-23269, Jan. 31, 1991.

[4]A. Granon, P. Goeuriot, and F. Thevenot, "Aluminum Magnesium Oxynitride: A New Transparent Spinel Ceramics," *J. Eur. Ceram. Soc.*, **15**, 249–54 (1995).

[5]D. Clay, D. Poslusny, M. Flinders, S. D. Jacobs, and R. A. Cutler, "Effect of $LiAl_5O_8$ Addition on the Sintering and Optical Transparency of LiAlON," *J. Eur. Ceram. Soc.*, **26**, 1351–62 (2006).

[6]T. M. Hartnett, R. L. Gentilman, and E. A. McGuire, "Aluminum Oxynitride having Improved Optical Characteristics and Method of Manufacture"; U.K. Pat. No. 2 169 270 A, Jul. 9, 1986.

[7]J. H. Lee, B. K. Koo, K. H. Koo, and K. R. Lee, "Method for Manufacturing Transparent Polycrystalline Aluminum Oxynitride"; WO Pat. No. 2008/047955 A1, April. 24, 2008.

[8]F. Zhang, S. W. Wang, Z. Zhang, and X. Y. Yuan, "Preparation of AlON Powder and Sintering of Transparent Ceramics," *Rare Met. Mater. Eng.*, **38**, 403–6 (2009).

[9]J. W. McCauley and N. D. Corbin, "Phase Relations and Reaction Sintering of Transparent Cubin Aluminum Oxynitride Spinel (AlON)," *J. Am. Ceram. Soc.*, **62**, 476–9 (1979).

[10]W. Rafaniello and I. B. Cutler, "Preparation of Sinterable Cubic Aluminum Oxynitride by the Carbothermal Nitridation Method of Aluminum Oxide," *J. Am. Ceram. Soc.*, **64**, C-128 (1981).

[11]S. Bandyopadhyay, G. Rixecker, F. Aldinger, S. Pal, K. Mukherjee, and H. S. Maiti, "Effect of Reaction Parameters on γ-AlON Formation from Al_2O_3 and AlN," *J. Am. Ceram. Soc.*, **85**, 1010–2 (2002).

[12]J. Qi, J. Zhou, W. Pang, J. He, Y. Su, Z. Liao, D. Wu, and T. Lu, "Study on the Preparation of AlON Powder by Solid State Reaction Method," *Rare Met. Mater. Eng.*, **36**, 88–91 (2007).

[13]X. Yuan, X. Liu, F. Zhang, and S. Wang, "Synthesis of γ-AlON Powders by a Combinational Method of Carbothermal Reduction and Solid-State Reaction," *J. Am. Ceram. Soc.*, **93**, 22–4 (2010).

[14]J. Zheng and B. Forslund, "Carbothermal Synthesis of Aluminum Oxynitride (AlON) Powder: Influence of Starting Materials and Synthesis Parameters," *J. Eur. Ceram. Soc.*, **15**, 1087–100 (1995).

[15]H. X. Willems, M. M. Hendrix, R. Metselaar, and G. D. With, "Thermodynamics of AlON: Stability at Lower Temperature," *J. Eur. Ceram. Soc.*, **10**, 327–37 (1992).

[16]Q. Shi, H. Liang, D. Feng, J. Wang, and G. D. Stucky, "Porous Carbon and Carbon/Metal Oxide Microfibers with Well-Controlled Pore Structure and Interface," *J. Am. Chem. Soc.*, **130**, 5034–5 (2008).

[17]L. Miller and W. D. Kaplanw, "Solubility Limits of La and Y in Aluminum Oxynitride at 1870°C," *J. Am. Ceram. Soc.*, **91**, 1693–6 (2008).

[18]S. S. Jada, "The Structure of Urea-Formaldehyde Resins," *J. Appl. Polym. Sci.*, **35**, 1573–92 (1988).

[19]D. K. Raval, B. N. Narola, and A. J. Patel, "Synthesis, Characterization and Composites from Resorcinol-Urea-Formaldehyde-Casein Resin," *Iran. Polym. J.*, **14**, 775–84 (2005).

[20]A. Boumaza, L. Favaro, J. Ledion, G. Sattonnay, J. B. Brubach, P. Berthet, A. M. Huntz, P. Royc, and R. Tetot, "Transition Alumina Phases Induced by Heat Treatment of Boehmite: An X-ray Diffraction and Infrared Spectroscopy Study," *J. Solid State Chem.*, **182**, 1171–6 (2009).

[21]J. H. Cantrell, "Determination of Absolute Bond Strength from Hydroxyl Groups at Oxidized Aluminum-Epoxy Interfaces by Angle Beam Ultrasonic Spectroscopy," *J. Appl. Phys.*, **96**, 3375–81 (2004).

[22]B. N. Dudkin, V. P. Krivoshapkin, and E. F. Krivoshapkina, "Effect of Aluminum Oxide Nanoparticles on the Properties of Urea-Formaldehyde Resin," *Russ. J. Appl. Chem.*, **79**, 1522–5 (2006).

[23]B. N. Dudkin, P. V. Krivoshapkin, and V. G. Luksha, "Synthesis of Aluminum Oxide Nanoparticles in an Aqueous Ammonium-Formaldehyde Solution," *Colloid J.*, **68**, 46–50 (2006).

[24]X. Jiang, C. Li, Y. Chi, and J. Yan, "TG-FTIR Study on Urea-Formaldehyde Resin Residue During Pyrolysis and Combustion," *J. Hazard. Mater.*, **173**, 205–10 (2010).

[25]I. M. Arafa, M. M. Fares, and A. S. Barham, "Sol–Gel Preparation and Properties of Interpenetrating, Encapsulating and Blend Silica-Based Urea-Formaldehyde Hybrid Composite Materials," *Eur. Polym. J.*, **40**, 1477–87 (2004).

[26]T. M. Hartnett, S. D. Bernstein, E. A. Maguire, and R. W. Tustison, "Optical Properties of AlON (Aluminum Oxynitride)," *Infrared Phys. Tech.*, **39**, 203–11 (1998).

[27]R. Apetz and M. P. van Bruggen, "Transparent Alumina: A Light Scattering Model," *J. Am. Ceram. Soc.*, **86**, 480–6 (2003).

[28]X. J. Liu, X. Y. Yuan, F. Zhang, Z. R. Huang, and S. W. Wang, "Fabrication of Aluminum Oxynitride Transparent Ceramics by Carbothermal Reduction Nitridation Processing," *J. Inorg. Mater.*, **25**, 678–82 (2010). □